Hybrid Beamforming for Satellite Ground Stations in the mmWave Band

Amélia Struyf*, Nédid Ismaili*, Philippe De Doncker*, Dimitri Lederer†, François Quitin*
*: Brussels School of Engineering, Univeristé Libre de Bruxelles, Brussels, Belgium, amelia.struyf@ulb.be
†: ICTEAM, UCLouvain, Louvain-la-Neuve, Belgium, dimitri.lederer@uclouvain.be

***Abstract*—One promising approach to increase data rates in satellite communication systems is using millimeter-wave (mmWave) communications. Ground stations (GSs) with mmWave antenna arrays offer high signal gains and more flexibility than traditional parabolic antennas. However, design costs of mmWave systems do not allow for fully-digital antenna arrays, where each antenna has its own Radio-Frequency (RF) chain. Instead, hybrid beamforming architectures, combining digital and analog beamforming, are preferred. In this paper, we present a low-complexity hybrid beamforming algorithm for GSs that relies on the knowledge of the satellites directions. We benchmark the rate performance of this method in a multi-satellite Multiple-Input Multiple-Output (MIMO) scenario and provide a comparison with more complex hybrid beamforming design methods. Simulation results show that the performance of the proposed geometrical algorithm approaches the performance of more complex state-of-the-art methods. Moreover, we present an experiment using mmWave Software-Defined Radios (SDRs) to validate the geometrical hybrid beamforming approach.**

***Index Terms*—satellite communications, hybrid beamforming, ground station, millimeter-wave.**

I. Introduction

To benefit from higher bandwidths, satellite communication systems increasingly shift towards higher frequency ranges, including the millimeter-wave (mmWave) spectrum. However, the cost of fully-digital multiantenna arrays with mmWave technology becomes prohibitive for large antenna arrays. In practice, antenna arrays operating in the mmWave bands typically use a hybrid analog-digital beamforming architecture, which requires a joint optimization of analog phase shifters and digital baseband signal processing [1].

Most research on hybrid beamforming for satellite communications has been focused on the satellite side, and little attention has been given to using hybrid beamforming architectures in ground stations (GSs), which are typically equipped with high-gain parabolic antennas. Compared to parabolic antennas, antenna arrays at GSs offer the advantages of faster beam steering and greater flexibility, including the ability to track multiple satellites simultaneously, an important feature in the context of current satellite mega-constellations [2], [3].

Hybrid beamforming architectures can be fully-connected or partially-connected. In fully-connected architectures, each Radio-Frequency (RF) chain is connected to all antennas while in partially-connected architectures each RF chain is connected to a different subset of antennas. Although the fully-connected architecture has been studied more extensively, partially-connected architectures are preferred for practical applications due to their smaller number of phase shifters and lower energy consumption [1], [4]. Solving partially-connected hybrid beamforming optimization problems requires addressing the joint analog-digital optimization. Current literature, mainly focused on 5G, presents solutions that tend to be computationally expensive [4]–[6]. However, due to the rapid satellite revolutions around the Earth, especially in low Earth orbits (LEO), these complex approaches may not be the most effective solutions. Moreover, most of the hybrid beamforming literature is focused on simulations-based studies, with limited experimental work conducted so far.

In this paper, we benchmark performances obtained by a LEO satellite GS equipped with a Ka-band antenna array with a partially-connected hybrid architecture in a multi-satellite Multi-Input Multi-Output (MIMO) scenario. We present a low-complexity geometrical approach to solve the joint analog-digital optimization problem based on the knowledge of the satellites directions. We compute channel rates obtained with the geometrical approach based on Starlink Two-Line Elements (TLE) data and compare them with other well-known partially-connected hybrid beamforming algorithms commonly studied for 5G applications. Moreover, an experiment is performed to validate the geometrical hybrid beamforming algorithm on data generated using a mmWave Software-Defined Radios (SDRs) system which implements a Ka-band hybrid analog-digital architecture.

Contributions: The main contributions of this paper can be summarized as follows:

- We propose a low-complexity hybrid beamforming algorithm for mmWave systems, that relies on the knowledge of the satellites directions;
- The proposed algorithm is benchmarked with other hybrid beamforming algorithms, and shows performance close to one of more complex algorithms;
- The proposed algorithm is validated on a mmWave SDR testbed.

The remainder of this paper is structured as follows. The system and channel model are presented in Section II, the geometrical hybrid beamforming design method is presented in Section III, the simulations results are presented in Section IV, the experiment is described in Section V and the paper is concluded in Section VI.

Notations: Uppercase bold letters $\mathbf{A}$ indicate matrices and lowercase bold letters $\mathbf{a}$ indicate vectors. The notation

$\cdot$ indicates a dot product. The terms ^{H}, *, and ^{T} represent the hermitian, complex conjugate, and transpose, respectively.

II. System and channel model

A. Signal model

Fig. 1 illustrates the system topology under consideration, showing the downlink transmission from multiple LEO satellites to a GS. The transmitting satellites are each equipped with a half-wavelength spaced uniform planar array (UPA) using an analog beamforming architecture with N_t antennas. The receiving GS is equipped with a half-wavelength spaced planar array using a hybrid analog-digital architecture with N_r antennas. The analog stage consists of fixed-amplitude phase shifters, assumed to have an infinite resolution. We consider a partially-connected architecture where each subset of N_{sub} antennas is connected to a single RF chain, such that the total number of RF chains N_{RF} corresponds to the number of satellites N_s.

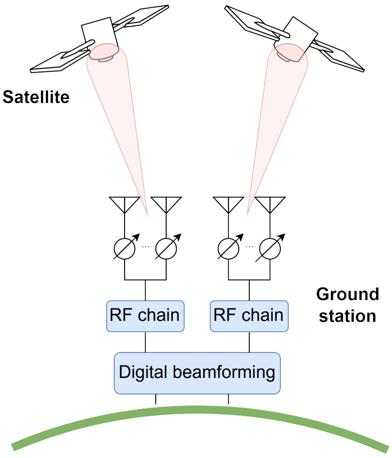

Fig. 1. Proposed system model. The number of subarrays at the GS is equal to the number of satellites.

Let us consider $\mathbf{s} \in \mathbb{C}^{N_s \times 1}$ which contains the symbols transmitted by the N_s satellites and $\mathbf{H} = [\mathbf{h}_1, \mathbf{h}_2, ..., \mathbf{h}_{N_s}] \in \mathbb{C}^{N_r \times N_s}$ which is the channel matrix from the satellites to each antenna of the GS. The received symbols after combining $\mathbf{y} \in \mathbb{C}^{N_s \times 1}$ are given by

$$\mathbf{y} = \mathbf{W}_{BB}^H \mathbf{W}_{RF}^H \mathbf{H}\mathbf{s} + \mathbf{W}_{BB}^H \mathbf{W}_{RF}^H \mathbf{n} \qquad (1)$$

where $\mathbf{W}_{BB} = [\mathbf{w}_{BB}^1, \dots, \mathbf{w}_{BB}^{N_s}] \in \mathbb{C}^{N_{RF} \times N_s}$ is the digital combiner and $\mathbf{W}_{RF}$ is the analog combiner having the following structure due to the partially-connected architecture considered:

$$\mathbf{W}_{RF} = \begin{bmatrix} \mathbf{w}_{RF}^1 & 0 & \cdots & 0 \\ 0 & \mathbf{w}_{RF}^2 & \cdots & 0 \\ 0 & 0 & \ddots & \vdots \\ 0 & 0 & \cdots & \mathbf{w}_{RF}^{N_s} \end{bmatrix} \qquad (2)$$

with $\mathbf{w}_{RF}^i \in \mathbb{C}^{N_{sub} \times 1}$ being the analog combiner vector of the i^{th} subset of antennas. The term $\mathbf{n} \in \mathbb{C}^{N_r \times 1}$ is the additive white Gaussian noise which is independent and identically distributed (i.i.d.) with a complex Gaussian distribution with zero mean and variance N_0 i.e. $\mathbf{n} \sim \mathcal{CN}(0, N_0)$.

B. Channel model

In the case of a multicarrier Orthogonal Frequency Division Multiplexing (OFDM) type communication system, each subcarrier can be modeled using a narrowband Line Of Sight (LOS) channel model. Multipath components are assumed to be negligible in such a scenario. We assume that the Doppler shift due to the movements of the satellites is compensated at the receiver and therefore negligible. Moreover, we assume that the satellites always have their beam perfectly directed towards the GS with a maximum gain $G_s = N_t G_0$ where G_0 is the gain of a single antenna element in both the GS and satellite antenna arrays.

The channel $\mathbf{h}_i$ between the satellite i and the GS can be written as:

$$\mathbf{h}_i = \alpha_i \mathbf{a}_r(\theta_i, \phi_i) e^{j\gamma_i} \qquad (3)$$

where $\alpha_i = L_{fs} L_{atm} \sqrt{G_s}\sqrt{G_0}$ includes the attenuation due to the free space path loss L_{fs} and the atmospheric attenuation L_{atm}, γ_i represents a random phase shift (comprising the effects of propagation, transceivers phase shifts, etc.) and $\mathbf{a}_r(\theta, \phi) \in \mathbb{C}^{N_r \times 1}$ is the receiver array steering vector defined as $\mathbf{a}_r(\theta, \phi) = \left[1, e^{-j\mathbf{k}\cdot\mathbf{r}_2}, \dots, e^{-j\mathbf{k}\cdot\mathbf{r}_{N_r}}\right]^T$ with $\mathbf{r}_n = \left[r_{n_x}, r_{n_y}\right]$ being the position of the n^{th} antenna along the x and y directions and $\mathbf{k} = \left[\frac{2\pi}{\lambda}\sin\theta\cos\phi, \frac{2\pi}{\lambda}\sin\theta\sin\phi\right]$ being the wave vector. λ, θ and ϕ are respectively the wavelength, the elevation, and the azimuth angles. A satellite is considered to have an elevation of $\theta = 0°$ when it is at the zenith of the GS and $\theta = 90°$ when it is at its horizon.

The atmospheric attenuation values used in this study were derived from models given in the ITU recommendations. The main cause of atmospheric attenuation is due to rain [7]–[9]. The other sources of attenuation considered are clouds attenuation [10], gaseous attenuation [11], and tropospheric scintillation [7].

III. Hybrid beamforming algorithms

This section presents the geometrical hybrid beamforming algorithm and two other state-of-the-art design methods, the Alterning minimization (Alt-min) and the Minimum Mean Square Error Successive Interference Cancellation (MMSE-SIC) beamforming, both widely studied for 5G applications.

A. Geometrical method

The geometrical method uses the direction of the satellites to find the combiner weights. This method is inspired by [12] which presents a hybrid beamforming design strategy for aerial networks. The direction-based beamforming algorithm is implemented in two stages: analog and digital weight computation.

1) Analog combining weights: The analog combining weights are computed based on the elevation θ and azimuth ϕ angles of each satellite such that each subarray beam of the GS is pointing exactly towards the direction of a different satellite. They are normalized to ensure that the gain of the system is unitary [12]:

$$\mathbf{w}_{RF}^{i} = \frac{\mathbf{a}_{r_i}^{*}(\theta_i, \phi_i)}{\sqrt{\frac{1}{4\pi}\int_0^{2\pi}\int_0^{\pi} |\mathbf{AF}(\theta,\phi)|^2 \sin\theta \, d\theta \, d\phi}} \tag{4}$$

where $\mathbf{a}_{r_i}$ are the N_{sub} components of $\mathbf{a}_r$ corresponding to the i^{th} subset of antennas and $\mathbf{AF}(\theta, \phi)$ is the array factor given by $\mathbf{AF}(\theta, \phi) = \mathbf{a}_{r_i}^{H}(\theta_i, \phi_i)\mathbf{a}_{r_i}(\theta, \phi)$.

2) Digital Combining: In the digital step, the interference is canceled to retrieve the different streams transmitted by the satellites. First, the equivalent baseband channel is computed as

$$\mathbf{H}_{eq} = \mathbf{W}_{RF}^{H}\mathbf{H}. \tag{5}$$

Then, a common digital minimum mean square error (MMSE) combiner is used for interference cancellation. The MMSE combiner allows one to cancel interference signals while taking the SNR into account [13]. The digital weights are computed as follows:

$$\mathbf{W}_{BB}^{H} = (\mathbf{H}_{eq}^{H}\mathbf{H}_{eq} + \frac{N_0}{P}\mathbf{I})^{-1}\mathbf{H}_{eq}^{H} \tag{6}$$

where P is the power transmitted by each satellite.

B. Alterning Minimization

The Alt-min algorithm for partially-connected architectures aims to approximate an optimal combiner (i.e. the combiner of a fully-digital system) by separating the combiner design into an analog and a digital design stage. It provides an optimal solution for each of these subproblems. This design approach is iterative, with the algorithm alternately optimizing the analog and digital combiners at each step. A detailed description of the algorithm can be found in [5].

C. MMSE-SIC

In MMSE-SIC, analog combiners are designed by dividing the analog combiner design problem into a series of simple problems, each only considering one subset of antennas. The optimal combiner for each subset is found by performing a singular value decomposition (SVD), as explained in [6]. For the digital stage, the equivalent baseband channel is first computed similarly to (5), and then the MMSE combiner (6) is applied.

Note that both the Alt-min and the MMSE-SIC algorithms require knowledge of the full channel matrix $\mathbf{H}$ (including any phase offset in the transmitter and receiver hardwares), whereas the geometrical algorithm only requires knowledge of the equivalent baseband channel, i.e. the channel after combining in the analog stage. The complexities of the different algorithms are presented in Table I, which shows that the proposed geometrical algorithm has a lower computational complexity compared to Alt-min and MMSE-SIC.

TABLE I

COMPARISON OF THE COMPUTATIONAL COMPLEXITY OF THE DIFFERENT METHODS. N_{iter} CORRESPONDS TO THE NUMBER OF ITERATIONS OF THE ALT-MIN ALGORITHM.

Design method	Computational Complexity
Geometrical	$\mathcal{O}(N_{sub}N_{RF}^3)$
Alt-min	$\mathcal{O}(N_{iter}N_{sub}N_{RF}^3)$
MMSE-SIC	$\mathcal{O}(N_{sub}^3N_{RF}^3)$

IV. SIMULATIONS

A. Simulation setup

The performance of the hybrid beamforming methods is evaluated in a scenario involving a constellation of Starlink satellites. The azimuth, elevation, and orbit radius of the satellites are generated by propagating Starlink TLE data using the Simplified General Perturbations 4 (SGP4) algorithm [14]. We assume that the GS tracks up to $N_{s_{max}}$ satellites simultaneously below an elevation angle of θ_t degrees. Tracking is initiated when a satellite goes below the elevation angle θ_t and is maintained until the satellite exceeds this threshold. Satellites expected to reach lower elevation angles are prioritized within the tracking algorithm. The detailed simulation parameters are shown in Table II.

TABLE II

SIMULATION PARAMETERS.

Parameter	Value
RF Frequency f_{RF}	28 GHz
Maximum number of satellites $N_{s_{max}}$	8
Number of TX antennas N_t	32x32
Number of antennas per sub-array N_{sub}	8x8 UPA
Gain of a single antenna G_0	5.46 dB
Antenna type	isotropic
Power Transmitted by each satellite P	15 W
Noise variance N_0	-135 dBm
Earth station latitude lat and longitude lon	50.81°, 4.38°
Earth station height h	58.1 m
Exceedance probability of atmospheric attenuation p	0.01 %
Threshold tracking elevation angle θ_t	60°
Duration of tracking t_{tr}	12 h
Tracking interval δ_t	5 s

We evaluate the performance of the three algorithms presented in Section III. Moreover, we also compute the results obtained with digital MMSE beamforming and the geometrical method with an identity matrix for the digital step for comparison purposes.

The signal-to-interference-plus-noise ratio (SINR) is computed as

$$SINR_i = \frac{|\mathbf{w}_i^H\mathbf{h}_i|^2}{\sum_{k\neq i}^{N} |\mathbf{w}_i^H\mathbf{h}_k|^2 + |\mathbf{w}_i|^2 N_0} \tag{7}$$

where $\mathbf{W} = \mathbf{W}_{RF}\mathbf{W}_{BB} = [\mathbf{w}^1, \ldots, \mathbf{w}^{N_s}] \in \mathbb{C}^{N_r \times N_s}$ are the hybrid combining weights. The rate can be deduced from the SINR as follows:

$$R_i = \log_2(1 + SINR_i). \tag{8}$$

The two metrics used to evaluate the performance of the algorithms are the sum rate $R_s = \sum_{i=1}^{N_s} R_i$ and the per-user rate $R_u = \frac{R_s}{Ns}$.

B. Simulation results

The resulting sum and per-user rates are shown in Fig. 2. Several observations can be made: 1) The sum and per-user rates obtained with the MMSE-SIC and geometrical method are very close. For the geometrical method, the MMSE interference cancellation improves the results. The MMSE-SIC method outperforms the geometrical approach because of the additional degree of freedom provided by the SVD, as it does not constrain the phases to conventional beamforming weights as in the case of the geometrical approach. 2) The Alt-min method performs poorly because it tries to reconstruct the digital beam but does not target interference cancellation. 3) The per-user rates of both the geometrical approach and the MMSE-SIC increase slightly with the number of antennas, due to the interference cancellation and the additions of GS antennas with each new satellite which increases the diversity. The geometrical identity and Alt-min results show that without interference cancellation the per-user rate decreases when the number of satellites increases.

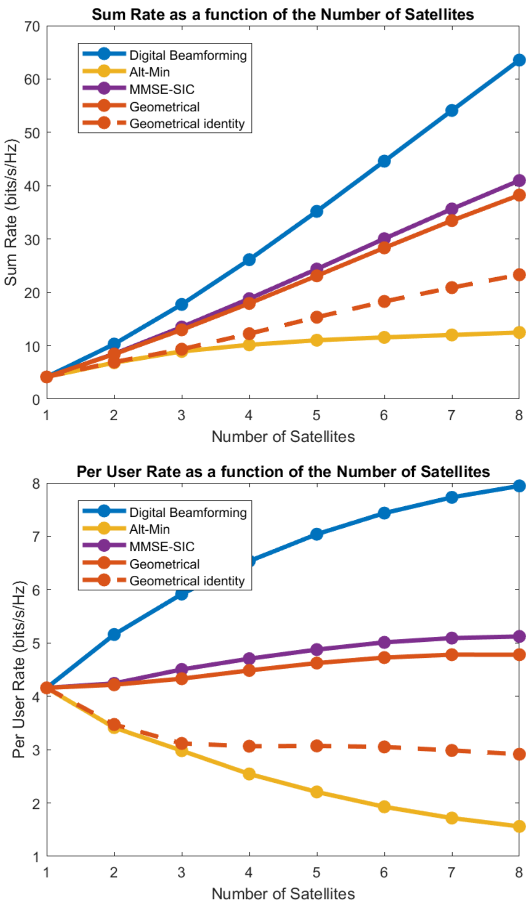

Fig. 2. Simulations results for the different algorithms. The geometrical approach performs very close to the MMSE-SIC algorithm.

V. Experiments

The geometrical hybrid beamforming algorithm is evaluated on an experimental setup for validation purposes. We first present the experimental setup and protocol, then we present the results. The experiment setup aims at reproducing the geometry of a typical satellite-to-ground scenario, with transmitters separated at angular spaces typical of a satellite scenario.

A. Experimental setup

The experimental setup used in this study is shown in Fig. 3. On the transmitter side, the system consists of a Universal Software-Defined Radio Peripherical (USRP) X310 SDR transmitting data packets on both its channels at a rate of 1 Msamples/s and an intermediate frequency of f_{IF} = 4 GHz. The USRP is connected to a dual-channel TMYTEK UDBox 5G up/down converter which up-converts the signals to a radio frequency of f_{RF} = 28 GHz. The UDBox is then connected to two TMYTEK BBox-One 5G beamformers, TX1 and TX2. On the receiver side, the signals are received by two BBoxes, RX1 and RX2, at f_{RF} and are down-converted to f_{IF} using a UDBox connected to a receiving USRP X310. TX1, TX2, RX1, and RX2 are each equipped with a 4x4 antenna array. To remove the carrier frequency offset, the local oscillators of the URSPs are synchronized by a 10 MHz octoclock, and the local oscillators of the UDBoxes are synchronized by outputting the 100 MHz clock of one UDBox and feeding it to the other. Both the transmitting and the receiving beamformers are positioned at an identical height. The transmitters are positioned at an angle of 10° relative to the boresight, such that $\theta_1 = -10°$ and $\theta_2 = 10°$ and the receivers are positioned side by side. TX1 and TX2 both transmit a different Quadrature phase-shift keying (QPSK) sequence. The usage of QPSK modulation has been chosen for simplicity purposes. The distance between the transmitters and receivers is 2.6 meters.

B. Experimental hybrid beamforming

The different stages of the experiments are as follows: first, the analog phase shifters are configured, then the equivalent baseband channel is estimated, and finally, digital combining weights are computed and applied to the received packets.

1) Analog beamforming: The BBoxes are configured such that the TX beams are steered at boresight and the RX1 and RX2 beams are respectively steered towards TX1 and TX2 by applying the phase shifts computed using (4).

2) H_{eq} estimation: The equivalent baseband channel H_{eq} is computed by doing a least square pilot-based estimation as [15]

$$\mathbf{H}_{eq}^{i,j} = (\mathbf{s}_p^H \mathbf{s}_p)^{-1} \mathbf{s}_p^H \mathbf{y}_p^{i,j} \tag{9}$$

where $\mathbf{s}_p$ corresponds to transmitted pilots, composed of Zadoff-Chu Long Term Evolution (LTE) Pulse-per-second (PSS) sequences, and $\mathbf{y}_p^{i,j}$ is the pilot received at RX$_i$ and transmitted by TX$_j$.

3) Digital combining: The digital combining weights are computed with (6) and are applied of the digital signals received at RX1 and RX2.

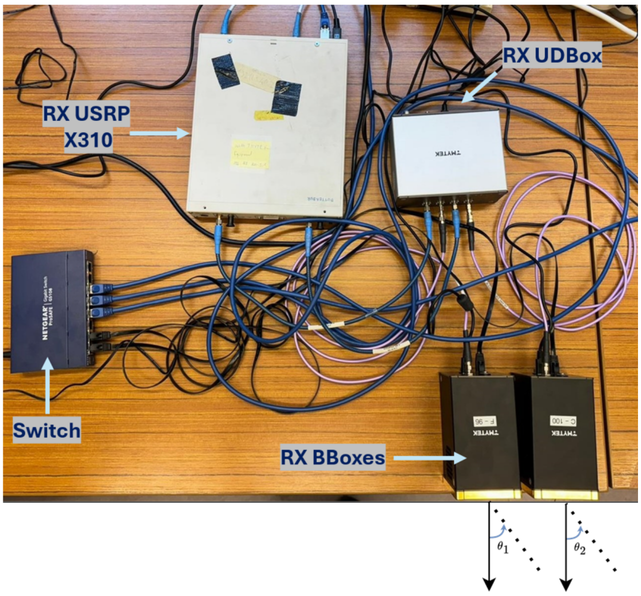

Fig. 3. Receiver experiment setup. A similar setup is used at the transmitter.

C. Experimental results

Fig. 4 shows the received baseband signals before and after digital combining. Before digital combining, the received constellation presents 16 points which correspond to the received signal of the targeted transmitter plus the interference of the other transmitter. Applying the digital combining weights allows one to remove the interferences and retrieve the transmitted signals with a perfect bit error rate (BER).

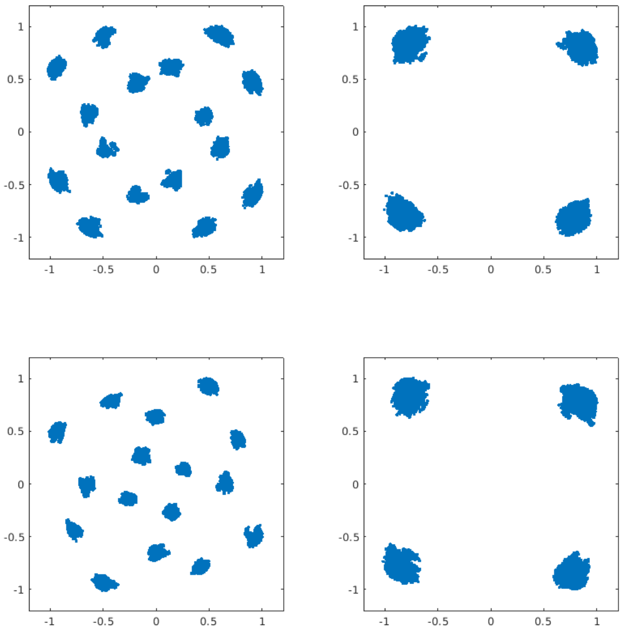

Fig. 4. Experimental results: The left subfigures show the received signals at RX1 and RX2 before digital combining, the right subfigures show the corresponding signals after digital combining.

VI. Conclusion

This paper benchmarks the rate performances that can be obtained using a plannar array as a GS antenna for satellite communications. It presents a low-complexity optimization approach for partially-connected architectures to follow one or multiple satellites and mitigate the interferences, which is more suitable than more complex methods in realistic satellite scenarios. Simulation results show that this simple approach successfully deals with interference and allows one to obtain results approaching those obtained with more computationally complex state-of-the-art algorithms. Moreover, the effectiveness of the geometrical approach based on the directions of the satellites has been demonstrated experimentally in a simple scenario with 2 satellites using a mmWave SDR system which implements a Ka-band hybrid analog-digital architecture.

Acknowledgment

The present research is part of the Space4ReLaunch project, which is supported by the SPW Economie Emploi Recherche of the Walloon Region, under the grant agreement nr 2210181.

References

[1] A. F. Molisch *et al.*, "Hybrid beamforming for massive mimo: a survey," *IEEE Communications Magazine*, vol. 55, no. 9, pp. 134–141, 2017.
[2] R. Sturdivantt and E. K. Chong, "System latency performance of mechanical and electronic scanned antennas for leo ground stations for iot and internet access," in *2017 Topical Workshop on Internet of Space (TWIOS)*, 2017, pp. 1–4.
[3] G. He, X. Gao, L. Sun, and R. Zhang, "A review of multibeam phased array antennas as leo satellite constellation ground station," *IEEE Access*, vol. 9, pp. 147 142–147 154, 2021.
[4] J. Zhang, X. Yu, and K. B. Letaief, "Hybrid beamforming for 5g and beyond millimeter-wave systems: a holistic view," *IEEE Open Journal of the Communications Society*, vol. 1, pp. 77–91, 2020.
[5] X. Yu, J.-C. Shen, J. Zhang, and K. B. Letaief, "Alternating minimization algorithms for hybrid precoding in millimeter wave mimo systems," *IEEE Journal of Selected Topics in Signal Processing*, vol. 10, no. 3, pp. 485–500, 2016.
[6] X. Gao, L. Dai, S. Han, C.-L. I, and R. W. Heath, "Energy-efficient hybrid analog and digital precoding for mmwave mimo systems with large antenna arrays," *IEEE Journal on Selected Areas in Communications*, vol. 34, no. 4, pp. 998–1009, 2016.
[7] ITU-R P.618-13, "Propagation data and prediction methods required for the design of earth-space telecommunication systems," 2017.
[8] ITU-R P.838-3, "Specific attenuation model for rain for use in prediction methods," 2005.
[9] ITU-R P.839-4, "Rain height model for prediction methods," 2013.
[10] ITU-R P.840-9, "Attenuation due to clouds and fog," 2023.
[11] ITU-R P.676-13, "Attenuation by atmospheric gases and related effects," 2023.
[12] T. Cuvelier and R. W. Heath, "Mmwave mu-mimo for aerial networks," in *2018 15th International Symposium on Wireless Communication Systems (ISWCS)*, 2018, pp. 1–6.
[13] Y. Jiang, M. K. Varanasi, and J. Li, "Performance analysis of zf and mmse equalizers for mimo systems: An in-depth study of the high snr regime," *IEEE Transactions on Information Theory*, vol. 57, no. 4, pp. 2008–2026, 2011.
[14] D. Vallado and P. Crawford, "Sgp4 orbit determination," in *AIAA/AAS Astrodynamics Specialist Conference and Exhibit*, 2008, p. 6770.
[15] S. Coleri, M. Ergen, A. Puri, and A. Bahai, "Channel estimation techniques based on pilot arrangement in ofdm systems," *IEEE Transactions on Broadcasting*, vol. 48, no. 3, pp. 223–229, 2002.